Structure and Dielectric Properties of Solid Solutions $Bi_7Ti_{4-x}Sn_xNbO_{21}$ (X = 0.0, 0.1, 0.2, 0.3, 0.4)

S. V. Zubkov and Y. A. Bulygin

Abstract The structural and electrophysical characteristics of a number of solid solutions of layered oxides of the perovskite-type $Bi_7Ti_{4-x}Sn_xNbO_{21}$ ($x = 0.0, 0.1, 0.2, 0.3, 0.4$) are studied. According to X-ray powder diffraction data, all the compounds studied are single-phase and have the structure of Aurivillius phases ($m = 2.5$) with a rhombic crystal lattice (space group I2cm, $Z = 2$). Changes in tetragonal and rhombic distortions of perovskite-like layers in compounds were considered depending on their chemical composition. The temperature dependences of the relative permittivity $\varepsilon(T)$ were measured. It was shown that the Curie temperature T_C of the perovskite-type oxides $Bi_7Ti_{4-x}Sn_xNbO_{21}$ ($x = 0.0, 0.1, 0.2, 0.3, 0.4, 0.5$) linearly decreases with increasing parameter x. The activation energies of charge carriers were obtained in different temperature ranges. It was found that there are three temperature regions with very different activation energies due to the different nature of the charge carriers in the studied compounds. The effect of substitution of Bi^{3+} ions by Sn^{4+} ions are investigated. It was found that for a number of compounds, the substitution of niobium ions by vanadium ions led to an increase in the dielectric constant and a decrease in the dielectric loss.

Keywords Layered perovskite-like oxides · Solid solutions · Aurivillius phases (APs) · Dielectric constant · Curie temperature

1 Introduction

Aurivillius phases (APs) [1–3] form a large family of bismuth-containing layered perovskite type compounds, with the chemical composition described by the general

S. V. Zubkov (✉)
Research Institute of Physics, Southern Federal University, 194, Stachki Ave., Rostov-on-Don 344090, Russia
e-mail: svzubkov61@mail.ru

Y. A. Bulygin
Department "International", Don State Technical University, 1, Gagarina, Rostov-on-Don 344090, Russia

I. A. Parinov et al. (eds.), *Physics and Mechanics of New Materials and Their Applications*, Springer Proceedings in Materials 10,
https://doi.org/10.1007/978-3-030-76481-4_16

formula $A_{m-1}Bi_2B_mO_{3m+3}$. The crystal structure of Aurivillius phases consists of alternating layers $[Bi_2O_2]^{2+}$, which are separated by m perovskite-like layers $[A_{m-1}B_mO_{3m+1}]^{2-}$, where A are the ions with large radii (Bi^{3+}, Ca^{2+}, Nd^{3+}, Sr^{2+}, Ba^{2+}, Pb^{2+}, Na^{+}, $K+$, Y^{3+}, Ln^{3+} (lanthanides)) have the dodecahedral coordination, whereas the B-positions inside oxygen octahedra are occupied by ions with small radii (Ti^{4+}, Nb^{5+}, Ta^{5+}, W^{6+}, Mo^{6+}, $Fe3^{+}$, Mn^{4+}, Cr^{3+}, Ga^{3+}, etc.). At present, considerable interest has been expressed in APs owing to potential practical applications associated with their extraordinary properties. APs are promising materials for use in the design and fabrication of high temperature piezoelectric sensors operating under extreme conditions. Moreover, these materials are considered as elements for nonvolatile ferroelectric random-access memory (FeRAM) devices [4, 5] and as multifunctional materials that exhibit magnetic properties (multiferroics) [6, 7], photoluminescence [8–10], etc. A substantial variability of the composition due to the substitution of A- and B-ions, as well as of the crystal structure due to variations in the number of layers $m = 1$–6, made it possible to obtain a large number of APs [11, 12]. A priority task is to determine correlations between the composition, structure, and dielectric characteristics of new APs. As was shown in our previous study [13], the modification of the composition of well-known APs by means of the addition of small amounts of donor dopants, such as W^{6+}, V^{5+}, Re^{7+}, and others, leads to a decrease in the number of oxygen vacancies, a decrease in the leakage current, and an improvement of the piezoelectric properties of APs ceramics. Moreover, there is an increase of the dielectric permittivity of the doped APs, as well as of their Curie temperature T_C, even though, to a lesser extent. For example, tungsten-doped SBT ceramics of the composition $SrBi_2$ $(W_xTa_{1-x})_2O_9$ ($x = 0$–0.2) demonstrated an increase in the remanent polarization with an increase in the tungsten concentration to $x \leq 0.075$ [14–18].

For APs $Bi_3Ti_{1-x}Sn_xNbO_9$, Zubkov et al. [19] investigated the effect of titanium tin substitution on the structure and dielectric properties. It was shown that the Curie temperature T_C increases and the maximum dielectric constant increases with increasing tin concentration. These changes in the dielectric characteristics of the APs were explained by a decrease in the tolerance factor for doped structures, since the Sn^{4+} ion has a larger ionic radius (0.69 Å for a coordination number (CN = 6) compared to Ti^{4+} ion (0.605 Å, CN = 6). The $Bi_7Ti_4NbO_{21}$ compound belongs to secondary APs with $m = 2.5$, in which layers of the initial APs with $m = 2$ (Bi_3TiNbO_9) and $m = 3$ ($Bi_4Ti_3O_{12}$) alternate regularly. This compound was previously found to have a higher remanent polarization compared to the two parent APs [20, 21].

In this work, we investigated the relationship between the structural characteristics and the electrophysical properties of a number of solid solutions APs $Bi_7Ti_{4-x}Sn_xNbO_{21}$ ($x = 0.0$, 0.1, 0.2, 0.3, 0.4) depending on the chemical composition. X-ray diffraction studies were carried out and the temperature dependences of the dielectric characteristics of new APs from the series: $Bi_7Ti_4NbO_{21}$, $Bi_7Ti_{3.9}Sn_{0.1}NbO_{21}$, $Bi_7Ti_{3.8}Sn_{0.2}NbO_{21}$, $Bi_7Ti_{3.7}Sn_{0.3}NbO_{21}$,

$Bi_7Ti_{3.6}Sn_{0.4}NbO_{21}$ were measured.

2 Experimental

Polycrystalline samples of APs were synthesized by the solid-phase reaction of the corresponding high purity oxides Bi_2O_3, SnO_2, TiO_2, Nb_2O_5. After weighting in accordance with the stoichiometric composition and a thorough grinding of the initial compounds with the addition of ethyl alcohol, the pressed samples were calcined at a temperature of 890 °C for 2 h. Then, the samples were repeatedly ground and pressed into pellets with a diameter of 10 mm and a thickness of 1.0–1.5 mm, followed by the final synthesis of APs at a temperature of 1120 °C (for 4 h). The X-ray diffraction patterns were recorded on a D2BRUKE diffractometer with a Cu X-ray tube. The Cu $K_{\alpha 1,\alpha 2}$ radiation was separated from the total spectrum with the use of a Ni-filter. The X-ray diffraction patterns were measured in the range of 2θ angles from 10° to 65° with a scan step of 0.02° and an exposure of 10 s per point. The analysis of the profiles of the diffraction patterns, the determination of the positions of the lines, their indexing (*hkl*), and refinement of the unit cell parameters were performed by using the PCW 2.4 program [22]. For dielectric permittivity and electrical conductivity measurements, on flat surfaces of APs samples in the form of disks with a diameter of 10 mm and a thickness of approximately 1 mm, electrodes were deposited using an Ag-Pd paste annealed at a temperature of 820 °C (for 1 h). The temperature and frequency dependences of the dielectric characteristics were measured using an E7-20 immittance meter in the frequency range from 100 kHz to 1 MHz and at temperatures in the range from room temperature to 900 °C.

3 Results and Discussion

Powder X-ray diffraction patterns of all investigated solid solutions $Bi_7Ti_{4-x}Sn_xNbO_{21}$ ($x = 0.1, 0.2, 0.3, 0.4$) correspond to single-phase APs with $m = 2.5$ and do not contain additional reflections. Figure 1 shows a powder X-ray diffraction pattern of a $Bi_7Ti_{4-x}Sn_xNbO_{21}$ ($x = 0.0, 0.1, 0.2, 0.3, 0.4$). It was found that all synthesized APs crystallize in an orthorhombic system with a unit cell space group I2cm (46).

(space group I2cm).

For the studied APs samples $Bi_7Ti_{4-x}Sn_xNbO_{21}$ ($x = 0.1, 0.2, 0.3, 0.4, 0.5$), the obtained unit cell parameters are close to those determined earlier: $a = 5.4469$ (4) Å, $b = 5.4121$ (4) Å, $c = 58.0429$ (47) Å [23]; $a = 5.45$ Å, $b = 5.42$ Å, $c = 58.1$ Å [24]; $a = 5.44$ Å, $b = 5.40$ Å, $c = 58.1$ Å [25]; $a = 5.442$ (1) Å, $b = 5.404$ (1) Å, $c = 57.990$ (12) Å (single crystal) [26]. The unit cell structure of APs $Bi_7Ti_4NbO_{21}$ can be described as the alternation of halves of the initial phases with $m = 2$ (Bi_3TiNbO_9) and $m = 3$ ($Bi_4Ti_3O_{12}$). It was previously found that this compound has a higher residual polarization compared to the two initial phases of Aurivillius along the *c*-axis, where the $BiTiNbO_7$ building blocks contain an equal amount of Ti^{4+} and Nb^{5+} ions in the perovskite layer and are separated.

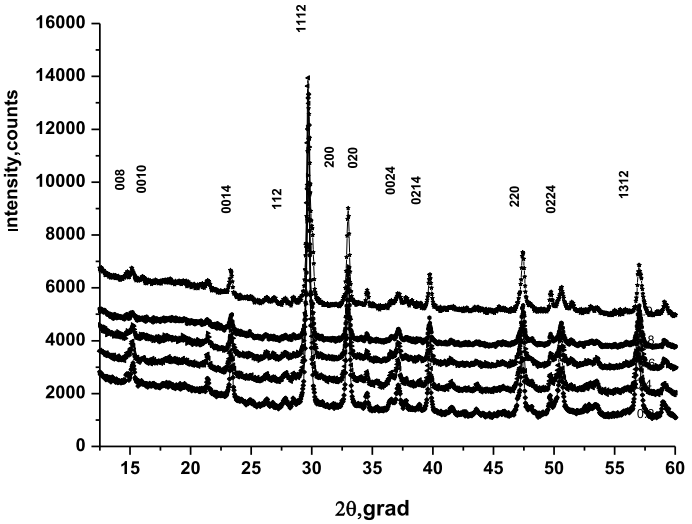

Fig. 1 X-ray powder diffraction patterns of $Bi_7Ti_{4-x}Sn_xNbO_{21}$ ($x = 0.0, 0.1, 0.2, 0.3, 0.4$)

These effects can also be associated with the partial ordering of atoms in the perovskite sublattice due to the significant difference in the radii of atoms located in the same positions in the perovskite layer. To obtain the degree of distortion of the ideal structure of perovskite in Gd^{3+}, we determined the tolerance coefficient t, which is presented in Table 1. The tolerance coefficient was introduced by Goldschmidt [27] as a parameter that determines the packing of ions in cubic unit cells:

$$t = (R_A + R_O)/2^{1/2}(R_B + R_O) \quad (1)$$

where R_A and R_B are the radii of cations in positions A and B, respectively; R_O is the ionic radius of oxygen. In this work, the tolerance coefficient t was calculatedtakinginto accountthe Shannon ionic radii offor the corresponding coordination numbers (CN) (O^{2-} (CN = 6) $R_O = 1.40$ Å, Sn^{4+} (CN = 6) $R_{Sn}{}^{4+} = 0.69$ Å, Nb^{5+} (CN = 6) $R_{Nb} = 0.64$ Å, Ti^{4+} (CN = 6) $R_{Ti} = 0.605$ Å). Shannon [28] did not provide the ionic radius of Bi^{3+} for coordination with CN = 12. Therefore, its

Table 1 Dielectric characteristics of $Bi_7Ti_{4-x}Sn_xNbO_{21}$ ($x = 0.0, 0.1, 0.2, 0.3, 0.4$)

	Compounds	t-factor	$\varepsilon/\varepsilon_0$ (T_1/T_2), 100 kHz	T_1, C	T_2, C	$E_1/E_2/E_3$, eV
1	$Bi_7Ti_4NbO_{21}$	0.973	1800/700	850	665	1.2/0.7/0.02
2	$Bi_7Ti_{3.9}Sn_{0.1}NbO_{21}$	0.972	1300/900	861	691	0.95/0.91/0.1
3	$Bi_7Ti_{3.8}Sn_{0.2}NbO_{21}$	0.9718	1350/1000	851	691	1.5/0.7/0.06
4	$Bi_7Ti_{3.7}Sn_{0.3}NbO_{21}$	0.971	1500/700	855	680	1.07/0.69/0.04
5	$Bi_7Ti_{3.6}Sn_{0.4}NbO_{21}$	0.97	1350/570	860	680	1.05/0.65/0.09

value was determined from the ionic radius with CN = 8 (R_{Bi} = 1.17 Å) multipliedby an approximation factor of 1.136, then for Bi^{3+} (CN = 12) we got R_{Bi} = 1.33 Å.

In addition to the results of structural studies, temperature dependences of the relative permittivity ε were obtained at various frequencies of 100–1000 kHz and various activation energies of charge carriers E_a in a wide temperature range. Figure 2 shows the temperature dependences of the relative permittivity $\varepsilon(T)$ and the loss tan

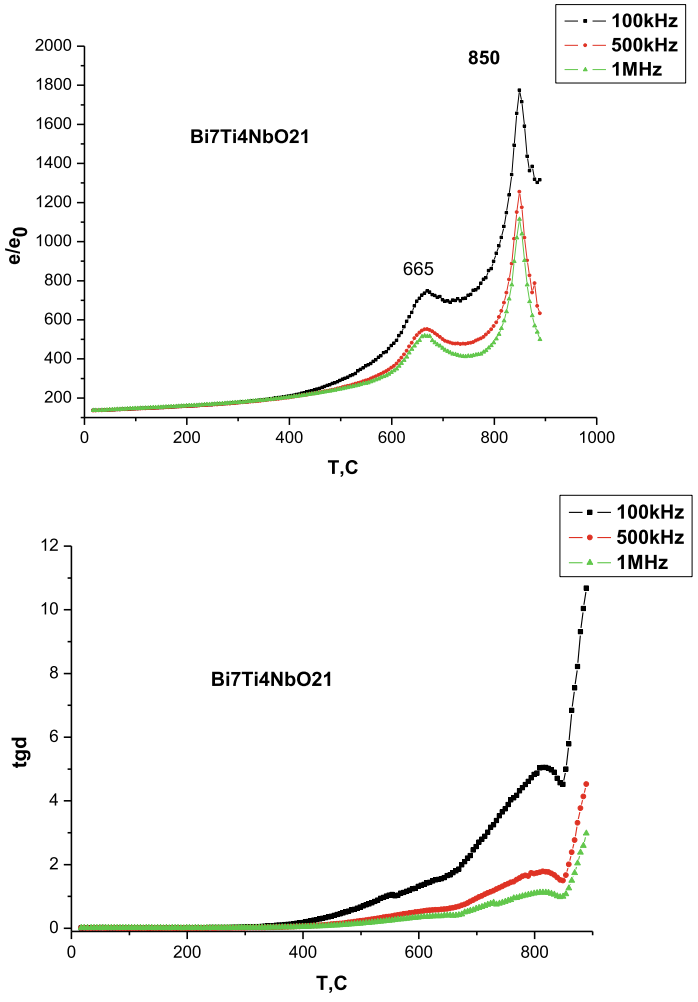

Fig. 2 Temperature dependences of the relative permittivity $\varepsilon/\varepsilon_0$ and the loss tan δ for APs $Bi_7Ti_{4-x}Sn_xNbO_{21}$ (x = 0.0, 0.1, 0.2, 0.3, 0.4) at a frequency of 100 kHz: $Bi_7Ti_4NbO_{21}$, $Bi_7Ti_{3.9}Sn_{0.1}NbO_{21}$, $Bi_7Ti_{3.8}Sn_{0.2}NbO_{21}$, $Bi_7Ti_{3.7}Sn_{0.3}NbO_{21}$, $Bi_7T_{3.6}Sn_{0.4}NbO_{21}$

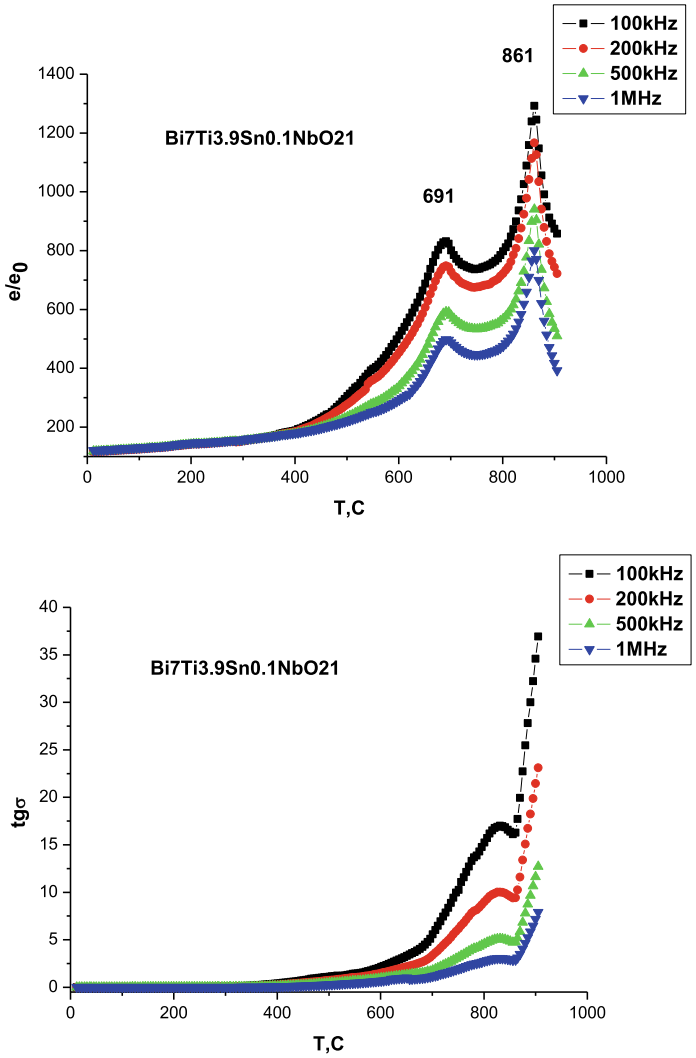

Fig. 2 (continued)

δ for $Bi_7Ti_{4-x}Sn_xNbO_{21}$ ($x = 0.0, 0.1, 0.2, 0.3, 0.4$) at a frequency of 100 kHz – 1 MHz. All $\varepsilon(T)$ dependences have two features at temperatures T_1 and T_2, for which the corresponding values of the permittivity are given in Table 1. The first peak on the $\varepsilon(T)$ dependence at temperature T_2 corresponds to the phase transition from the polar to the polar phase (ferroelectric–ferroelectric), this transition in the temperature range from T_1 to T_2 is accompanied by the removal of distortions for the $Bi_2Ti_3O_{10}$ perovskite block with $m = 3$, while in the $BiTiNbO_7$ perovskite layers with $m = 2$, the distortions of the octahedral layers are retained.

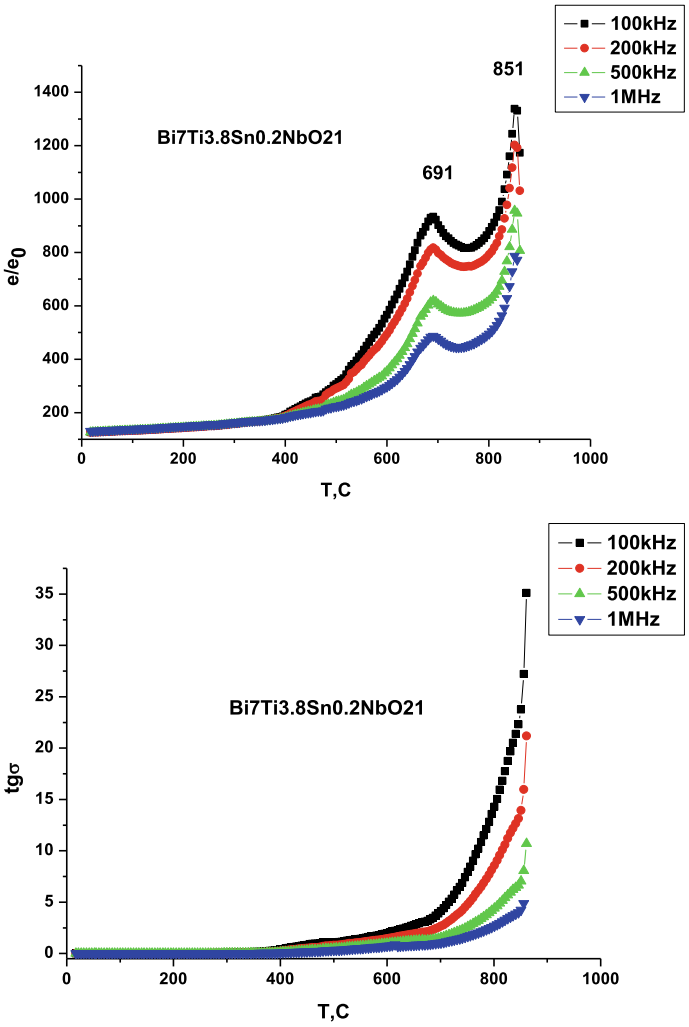

Fig. 2 (continued)

At temperatures above T_1, distortions are removed in both blocks of the perovskite type, and the Sn^{4+} symmetry is close to I4/mmm3. Thus, the temperature T_1 corresponds to the transition from the polar to the nonpolar phase (paraelectric–ferroelectric phase) those are the Curie temperature T_C. Replacement of B ions in Ti^{4+} octahedra by ions with a large ionic radius does not lead to significant changes in the dielectric characteristics of these compounds. Accordingly, one should not expect significant changes in the temperature T_1 from the tolerance coefficient t due to changes in the average radii of the ions B. Figure 2 shows the dependences of the temperatures T_1 and T_2 on the parameters x and t for $Bi_7Ti_{4-x}Sn_xNbO_{21}$,

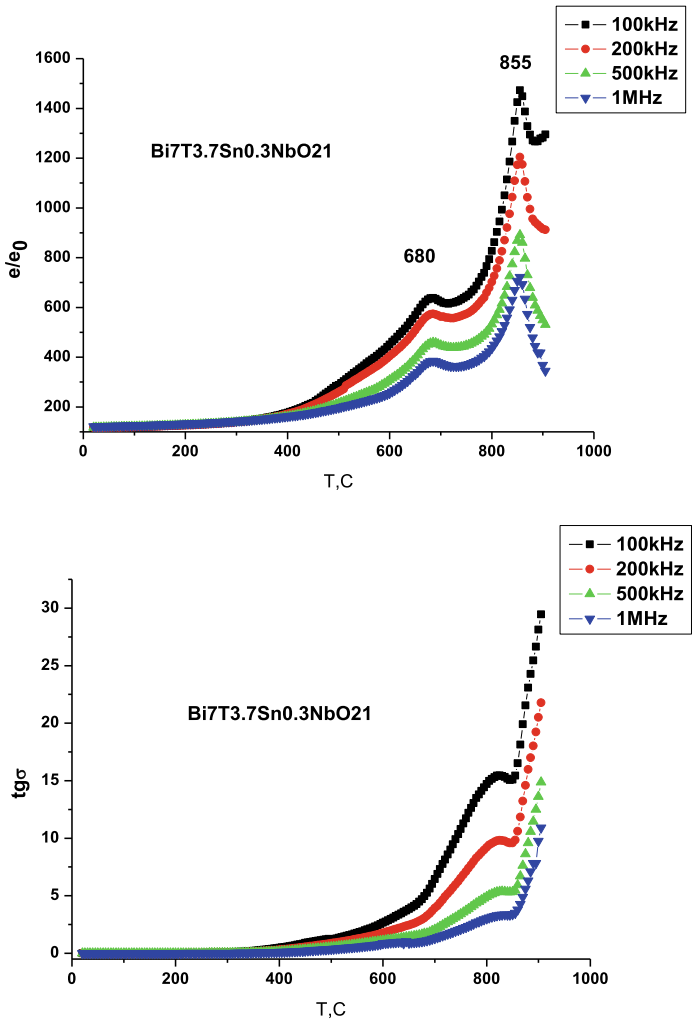

Fig. 2 (continued)

which turned out to be expected for this type of substitution. It should be noted that with an increase in the tin concentration, the increase in the temperature T_2 and T_1 is weakly expressed (it remains practically unchanged for T_1) compared to $T_2(x)$ (which increases by only about 25 °C for $x = 0.1, 0.2$. A possible explanation for the difference in the dependences $T_1(x)$ and $T_2(x)$ can be the assumption that the substitution of Ti^{4+} ions in octahedra for Sn^{4+} ions occur mainly not in the most distorted perovskite layer of $BiTiNbO_7$ with $m = 2$, but to a greater extent in a more symmetric compound $Bi_2Ti_3O_{10}$ with $m = 3$. The maxima on the temperature dependence of the permittivity $\varepsilon(T)$ show the dependence of m on the composition

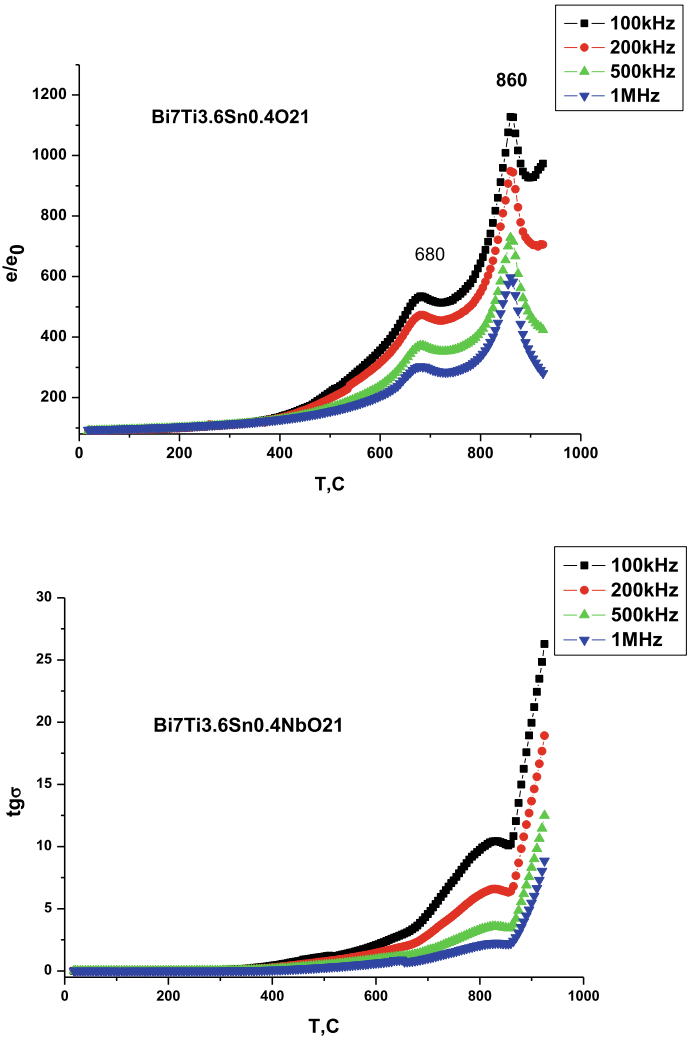

Fig. 2 (continued)

of $Bi_7Ti_{4-x}Sn_xNbO_{21}$ (Table 1). It should be noted that earlier dielectric studies of this system of solid solutions did not reveal any dependence. In our case, we observe a sharp jump in $\varepsilon/\varepsilon_0$ at T_2 for $x = 0.1, 0.2$. Since the dielectric constant $\varepsilon(T)$ depends on many factors (composition, grain size, porosity, concentration of vacancies, etc.), the combination of all these factors usually neutralizes this dependence. A significant increase in the dielectric constant can be explained by the size of the ionic radius, which differs from those previously used for doping. The obtained values of the dielectric loss tangent tan δ for $Bi_7Ti_{4-x}Sn_xNbO_{21}$ ($x = 0.1, 0.2, 0.3, 0.4$) are presented in Fig. 2. For all $Bi_7Ti_{4-x}Sn_xNbO_{21}$ ($x = 0.1, 0.2, 0.3, 0.4$), we observe an

increase in tan δ with increasing x. The obtained values of the activation energy E_a of charge carriers in $Bi_7Ti_{4-x}Sn_xNbO_{21}$ are presented in Table 1.

The activation energy E_a was determined from the Arrhenius equation:

$$\sigma = (A/T)\exp(-E_a/kT) \tag{2}$$

where σ is electrical conductivity, k is Boltzmann constant, and A is constant. A typical dependence of lnσ on $1/kT$ (at a frequency of 100 kHz), which was used to determine the activation energies E_a, is shown in Fig. 3 for the APs $Bi_7Ti_{4-x}Sn_xNbO_{21}$ ($x = 0.1, 0.2, 0.3, 0.4$).

Figure 3 clearly shows that there are three temperature regions, in which the activation energies E_a have significantly different values. For two high-temperature regions, characterized by high activation energies of charge carriers, the values $E_a(1) > E_a(2)$ differ from each other by almost 2 times, and the boundary of the change in the activation energy is close to the phase transition temperature T_1. It should be noted that the values of E_a corresponding to the electrical conductivity in a wide temperature range from 300 °C to T_2 systematically decrease with increasing doping with Nd^{3+} ions for all members of the $Bi_7Ti_{4-x}Sn_xNbO_{21}$ series, while in the high-temperature region above T_1 for E_a such a dependence is not observed. It is known [29] that, in a wide temperature range, the determining factor is ionic conductivity, which occurs by the mechanism of oxygen ions jumping into existing vacancies in the crystal lattice.

This intrinsic conductivity is characterized by relatively high charge carrier activation energies of approximately 1 eV. The doping of Sn^{4+} by different cations can lead to a change in their conductivity, both toward an increase with the formation of additional oxygen vacancies and toward a decrease, when these vacancies are bound with doped metal ions. The systematic decrease in the activation energy in the series of $Bi_7Ti_{4-x}Sn_xNbO_{21}$ with an increase in the concentration of Sn^{4+} ions,

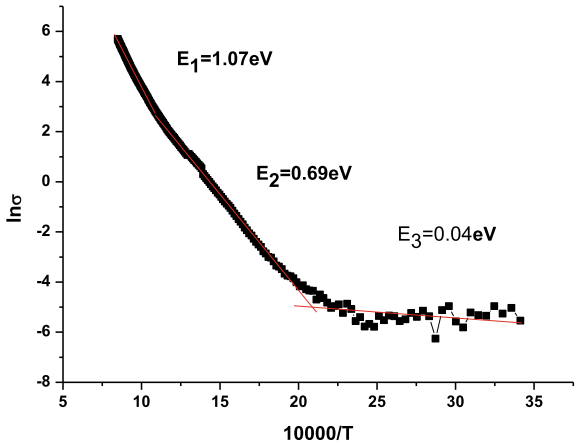

Fig. 3 Dependence of lnσ on 10,000/T for the $Bi_7Ti_{4-x}Sn_xNbO_{21}$ samples

which leads to an increase in the electrical conductivity, indicates the first mechanism of change in the electrical conductivity ofthese Sn^{4+}. The obtained values of for the studied series of $Bi_7Ti_{4-x}Sn_xNbO_2$ are close to the characteristic values of the activation energy (approximately 0.5–1.0 eV) for oxygen vacancies in the Sn^{4+}. The nature of the conductivity in APs at temperatures above T_2 with higher values of E_a (1) > 1.5 eV requires further investigation. In the low-temperature range, the electrical conductivity is predominantly determined by impurity defects with very low activation energies of the order of a few hundredths of an electron-volt.

4 Conclusion

A series of layered bismuth perovskite oxides $Bi_7Ti_{3.9}Sn_{0.1}NbO_{21}$, $Bi_7Ti_{3.8}Sn_{0.2}NbO_{21}$, $Bi_7Ti_{3.7}Sn_{0.7}NbO_{21}$, $Bi_7Ti_{3.6}Sn_{0.4}NbO_{21}$ were synthesized by the solid-state method. The X-ray diffraction studies carried out in our work showed that all the compounds obtained have the PP structure ($m = 2.5$) with an orthorhombic crystal lattice (space group I2cm, $Z = 2$). An analysis of the details of the APs structure showed that an increase in the concentration x of tin x from 0.1 to 0.4 and a partial replacement of bismuth ions with tin ions lead to an increase in the tangent of the dielectric loss angle and a decrease in $\varepsilon/\varepsilon_0$. The temperature dependences $\varepsilon(T)$ in the $Bi_7Ti_{4-x}Sn_xNbO_{21}$ compounds ($x = 0.2$–1.0) exhibit two anomalies: (i) the low-temperature anomaly corresponds to the ferroelectric phase transition, and (ii) the high-temperature anomaly isassociated with the Curie temperature T_C, which corresponds to the ferroelectric phase of the paraelectric transition. Ligation with tin ions (100%) does not lead to a significant shift in low temperature peaks.

Acknowledgements The study was financially supported by the Russian Science Foundation (Grant No. 21-19-00423).

References

1. B. Aurivillius, Arkiv. Kemi. **1**, 463 (1949)
2. B. Aurivillius, Arkiv. Kemi. **58**, 499 (1949)
3. B. Aurivillius, Kemi. **37**, 512 (1950)
4. B.H. Park, B.S. Kang, S.D. Bu, T.W. Noh, J. Lee, W. Jo, Nature (London) **401**, 682 (1999)
5. A.P. de Araujo, J.D. Cuchiaro, L.D. Mcmillan, M.C. Scott, J.F. Scott, Nature (London) **374**, 627 (1995)
6. X. Chen, J. Xiao, Y. Xue, X. Zeng, F. Yang, P. Su, Ceram. Int. **40**, 2635 (2014)
7. V.G. Vlasenko, V.A. Shuvaeva, S.I. Levchenkov, Y.V. Zubavichus, S.V. Zubkov, J. Alloys Compd. **610**, 184 (2014)
8. H. Zou, X. Hui, X. Wang, D. Peng, J. Li, Y. Li, X. Yao, J. Appl. Phys. **114**, 223103 (2013)
9. H. Nakajima, T. Mori, S. Itoh, M. Watanabe, Solid State Commun. **129**, 421 (2004)
10. F. Gao, G.J. Ding, H. Zhou, G.H. Wu, N. Qin, D.H. Bao, J. Electrochem. Soc. **158**(5), G128 (2011)

11. S.V. Zubkov, V.G. Vlasenko, V.A, J. Phys. Solid State, **58**(1), 44 (2016)
12. T. Wang, Hu. Jiacong, H. Yang, Li. Jin, X. Wei, C. Li, F. Yan, Y. Lin, J. Appl. Phys. **121**, 084103 (2017)
13. S.V. Zubkov, V.G. Vlasenko, J. Phys. Solid State. **59**(12), 2325 (2017)
14. I. Coondoo, S.K. Agarwal, A.K. Jha, Mater. Res. Bull. **44**, 1288 (2009)
15. I. Coondoo, N. Panwar, A. K. Jha, Physica B (Amsterdam). **406**, 374 (2011)
16. J.K. Kim, T.K. Song, S.S. Kim, J. Kim, Mater. Lett. **57**(4), 964 (2002)
17. W.T. Lin, T.W. Chiu, H.H. Yu, J.L. Lin, S. Lin, J. Vac. Sci. Technol. A **21**, 787 (2003)
18. Y. Wu, S.J. Limmer, T.P. Chou, C. Nguyen, G.Z. Cao, J. Mater. Sci. Lett. **21**, 947 (2002)
19. S.V. Zubkov**,** J. Advanced Materials, 231 (2020)
20. F. Chu, D. Damjanovic, J. Am. Ceram. Soc. **78**, 3142 (1995)
21. Z.G. Yi, Y. Wang, Y.X. Li, Q.R. Yin, J. Appl. Phys. **99**, 114101 (2006)
22. W. Kraus, G. Nolze, *PowderCell for Windows. Version 2.3* (Federal Institute for Materials Research and Testing, Berlin, 1999)
23. A. Yokoi, H. Ogawa, Mater. Sci. Eng. B **129**, 80 (2006)
24. S. Horiuchi, T. Kikuchi, M. Goto, Acta Crystallogr. Sect. A: Cryst. Phys. Diffr. Theor. Gen. Crystallogr. **33**, 701 (1977)
25. P. Duran, F. Capel, C. Moure, M. Villegas, J.F. Fernandez, J. Tartaj, A.C. Caballero, Eur. Ceram. Soc. **21**, 1 (2001)
26. D. Mercurio, Int. J. Inorg. Mater. **2**(5), 397 (2000)
27. V.M. Goldschmidt, *Geochemische Verteilungsgesetze Der Elemente* (Norske, Oslo, 1927).
28. R.D. Shannon, Acta Crystallogr. Sect. A: Cryst. Phys. Diffr. Theor. Gen. Crystallogr. **32**, 75 (1976)
29. A. Isupov, J. Neorg. Khim. **39**, 731 (1994)